

S-EVC Method for Sorting Wafers with Defects that Extend to Bar Shaped SSFs

Kazumi Takano^{1,a*}, Yasuyuki Igarashi^{1,b} and Yohsuke Matsushita^{1,c}

¹ITES, 1-60 Kuribayashi, Otsu, Shiga 520-2151, Japan

^akazumi_takano@ites.co.jp, ^byiga@ites.co.jp, ^cyohsuke_matsushita@ites.co.jp

Keywords: BPD (basal plane dislocation), SSF (Shockley-type stacking fault), PL (photoluminescence), UV Irradiation

Abstract. In the previous report [1], we proposed the S-EVC (Selective Expansion-Visualization-Contraction) method (Fig. 1) that effectively screens for malignant BPDs (basal plane dislocations) in the drift and buffer layers, which expand to SSFs (Shockley-type stacking faults), leading to forward voltage degradation. The method intentionally utilizes the REDG (recombination enhanced dislocation glide) mechanism by UV (ultraviolet) irradiation in wafer sorting to replace the so-called burn-in (accelerated current stress) process, which is time-consuming during mass production. In the report, triangular SSFs were examined to verify the effectiveness of the method, but they only occupy a much smaller area of the active region on the chip than bar shaped SSFs. In this study, to improve the S-EVC method to be more practical, we focused on the more serious bar shaped SSFs which have a non-negligible impact on electrical characteristics. The bar shaped SSFs are mostly expanded from TED (threading edge dislocation)-converted BPD at or below the substrate epitaxial layer interface [2]. In PL (photoluminescence) observation by a 710 nm LPF (long-pass filter), the TED-converted BPD and the complete TED extended from the bottom of the substrate are observed as the same dark spot, but it was confirmed that both can be distinguished by the presence or absence of their SSF expansion by UV irradiation. In addition, in order to confirm the validity of the S-EVC method even on the virgin epi wafer, UV irradiation was performed on both the aluminum doped PN structured wafer and the virgin epi wafer, and the similar SSF expansion was observed. Meanwhile, the correlation between UV irradiation and forward bias degradation was quantified using PiN diodes by comparing the glide velocity of 30°Si(g) core partials for bar shaped SSFs by UV irradiation stress with that by current stress.

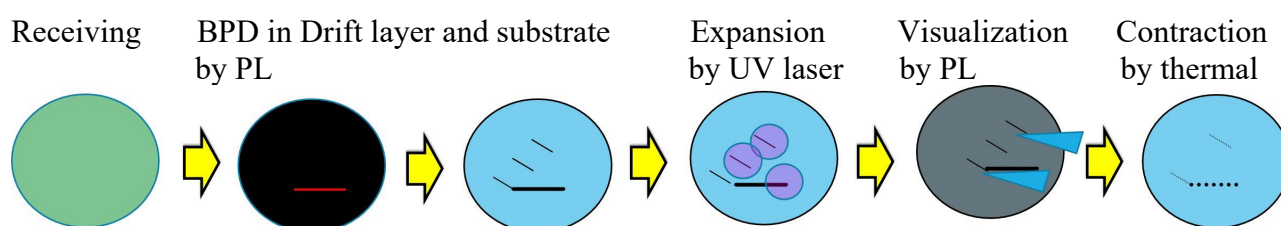


Fig. 1 The S-EVC (Selective Expansion-Visualization-Contraction) method

Introduction

Capital investment for mass production of SiC MOSFETs is underway around the world in preparation for the popularization and expansion of electric vehicles. 4H-SiC substrates still have a lot of BPDs, so SiC Schottky diodes must be incorporated into MOSFET modules as a forward bias degradation measure, which is costly. In the paper by Ishigaki et al. that investigated the forward bias degradation of approximately 10,000 SiC MOSFET modules, a 10 % increase in V(on) voltage was reported for 2-3% of the modules [3]. Kallinger et al. showed that BPDs inside epi-layer on 4H-SiC substrate were optically stressed by applying high UV laser irradiation, which can induce expand 1-SSF from the BPD at the wafer level similar to electrical burn-in testing [4]. Our proposed S-EVC method can detect not only the BPDs inside epi-layer but also the TED-converted BPDs that expand to bar shaped SSFs.

Experiments and Results

First, we have confirmed that UV irradiation can visualize and capture the TED-converted BPDs which may expand to bar shaped SSFs under forward bias operation. The sample investigated was a commercially available n-type 100 mm Φ 4H-SiC epi-wafer with a 4° off-cut angle, on which heavily nitrogen-doped buffer layer ($0.5\ \mu\text{m}$, $1 \times 10^{18}\text{cm}^{-3}$) and lightly doped drift layer ($11\ \mu\text{m}$, $6 \times 10^{15}\text{cm}^{-3}$) were epitaxially grown. We examined BPDs by UVPL (UV photoluminescence) observation through a 710 nm LPF (Fig. 2(a)). Dark spots are TEDs or TSDs (threading screw dislocations) in the epi layer. The TEDs, indicated by blue arrows, were the starting point of the bar shaped SSFs. Next, after UV laser irradiation ($355\ \text{nm}$, $186\ \text{W/cm}^2$) at the same location as in Fig. 2(a), the bar shaped SSFs were confirmed by UVPL observation through a 420 nm BPF (bandpass filter) (Fig. 2(b)). The white bright lines are the Si(g) core partials, the yellow lines added in the figure are the C(g) (carbon) core partials, and the blue lines are the interface between the epilayer and the substrate (Fig.2(c)). The point where the two (the yellow and the blue) lines intersect is the starting point of the bar shaped SSF [5]. The dark dots at the intersection are the TEDs converted from BPDs at the substrate-buffer layer interface. From these results, we were able to estimate the location of the C(g) core partials and identify the BPD as the starting point of the expansion.

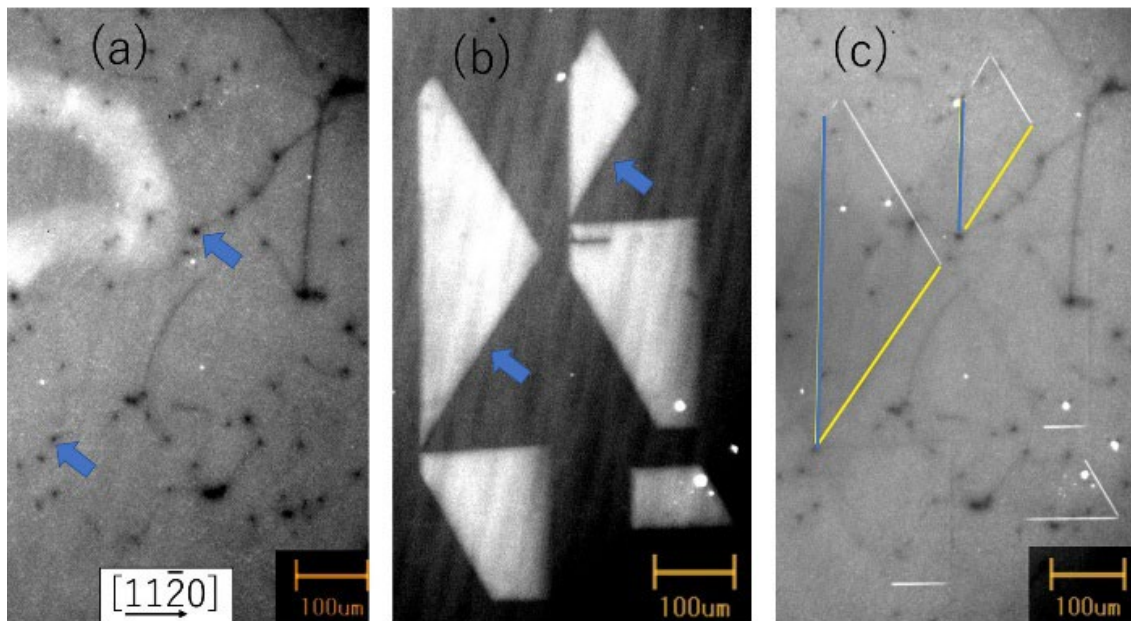


Fig. 2. (a) UVPL image of epi wafer through LPF (710 nm) after UV irradiation, (b) UVPL image through BPF (420 nm) and (c) UVPL image through LPF (710 nm).

To confirm that the TED-converted BPD at the substrate-epilayer interface is the starting point for SSF expansion, an etching test was performed. Fig.3 shows a schematic of the TED-converted BPD and extended SSF.

The blue arrow is TED converted from BPD and through the surface of the epilayer. The C(g) core dislocation extends from the BPD of the substrate in a line through the epilayer.

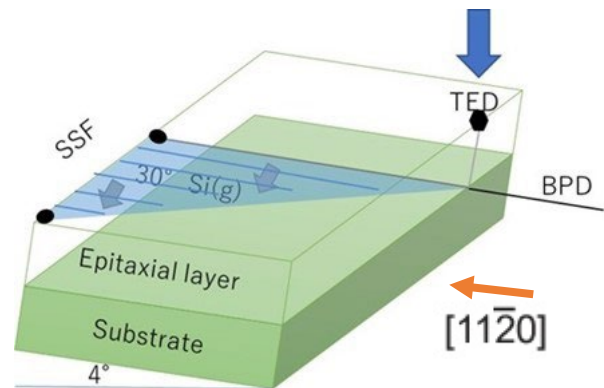


Fig. 3. Schematic diagram

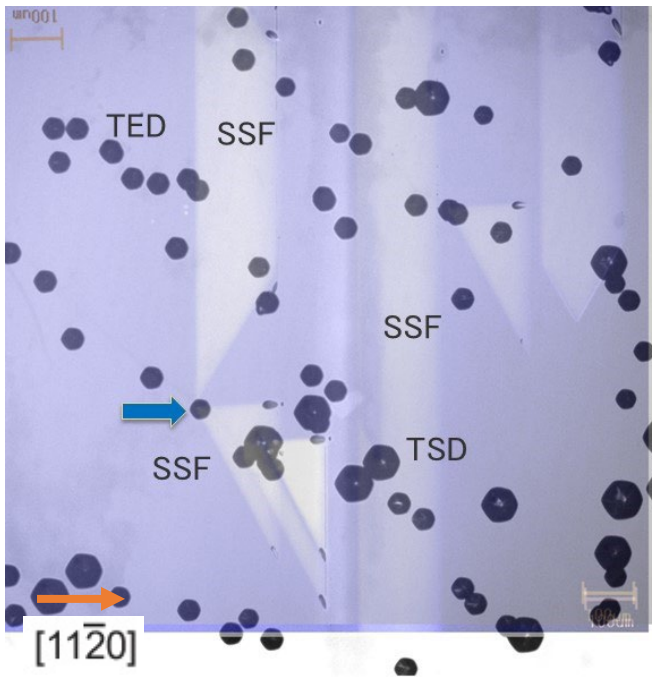


Fig. 4. Composite image

Next, the epilayer was entirely removed by polishing to expose the substrate, and the substrate surface was etched with molten KOH. If the TED (indicated by the blue arrow) in Fig. 4 was converted from a BPD, the tip of the BPD should be observed from this point, as shown in Fig. 5.

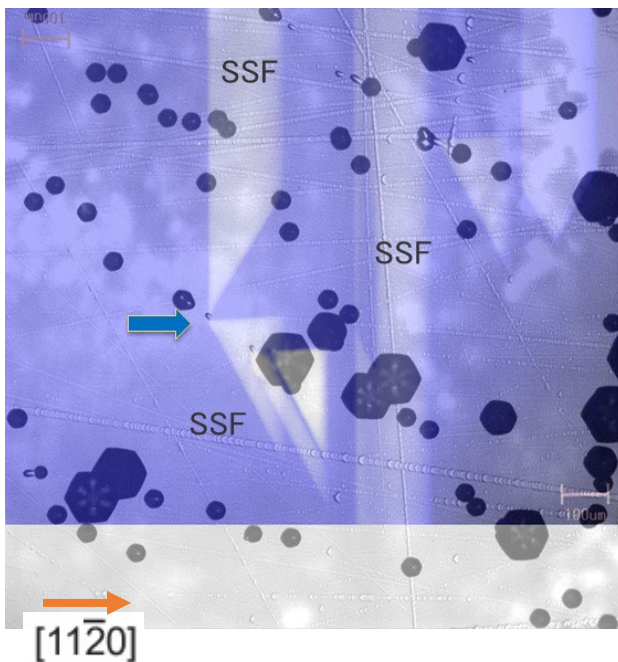


Fig. 6. Composite image after polishing

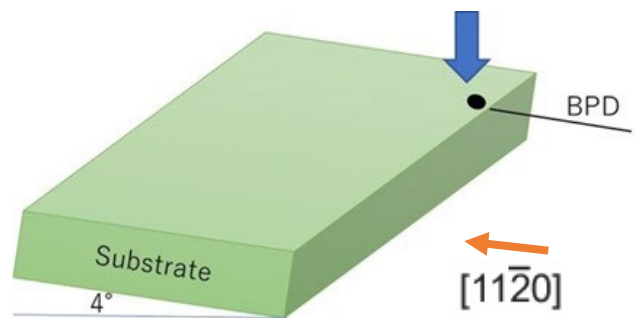


Fig. 5. Schematic diagram

Fig. 6 shows a composite image of the PL image overlaid with the etch pit photo after the epilayer was removed. A shell-shaped etch pit was observed at the point that was TED in Fig. 4 (blue arrow), and the shape of the BPD indicates that it was a BPD extending from the upper left 30° direction in the substrate. Therefore, this point was confirmed to be the BPD converted to TED at the epi/substrate interface and the starting point of the expansion to SSF.

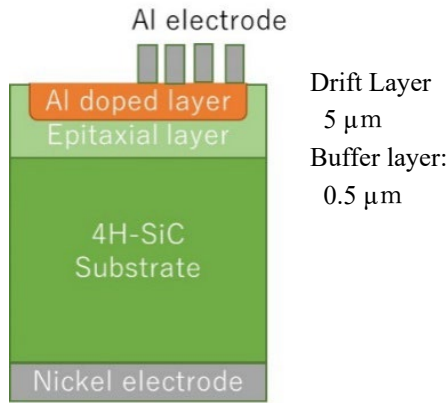
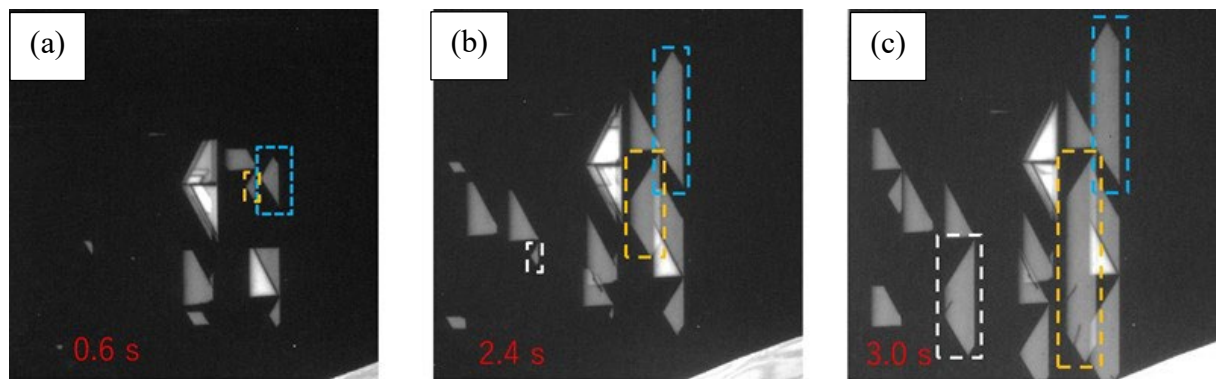


Fig. 7. Schematic cross section

Second, we fabricated PiN diodes and measured the expansion speed induced by UV irradiation. We also attempted to quantify the correlation between UV irradiation and current density by conducting forward bias testing using the same wafer. The sample of the PiN structure was formed by doping aluminum ($1 \times 10^{20} \text{ cm}^{-3}$) on the Si face of the epi wafer (buffer layer ($0.5 \mu\text{m}$, $1 \times 10^{18} \text{ cm}^{-3}$), drift layer ($5 \mu\text{m}$, $1 \times 10^{16} \text{ cm}^{-3}$)). A nickel electrode was then formed as backside Ohmic contacts, and an aluminum electrode array of comb pattern was formed in half the area of the Si face surface. The structure of the processed epi wafer is shown in Fig. 7.

Fig 8. Expanded SSFs in epi wafer at 186 W/cm^2

Both of the non-processed epi-wafer and the PiN structured wafer were UV irradiated and the length of the expanded SSFs was measured. The ultraviolet laser (355 nm) irradiation time is 0.6 s, 2.4 s and 3.0 s for (a), (b) and (c), respectively in Fig. 8. The glide velocity of 30°Si(g) core partials for bar shaped SSF was calculated from the time slope of the length, as seen in Fig. 9. Fig. 10 shows the relationship between the velocity and the UV irradiance. The faster expansion rate in the epi-wafer than in the PiN structure wafer was thought to be due to the easier surface recombination of carriers to the electrode, nickel, and their rapid disappearance.

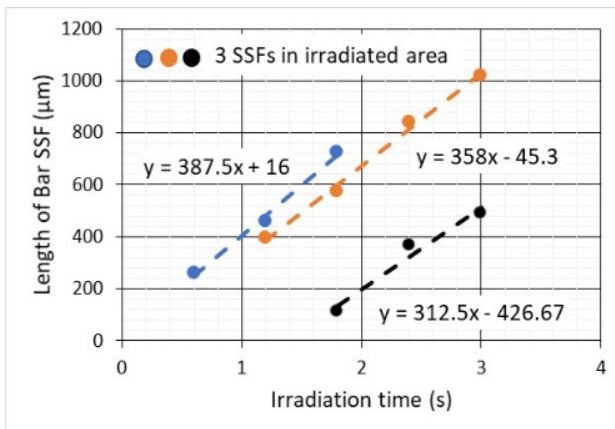
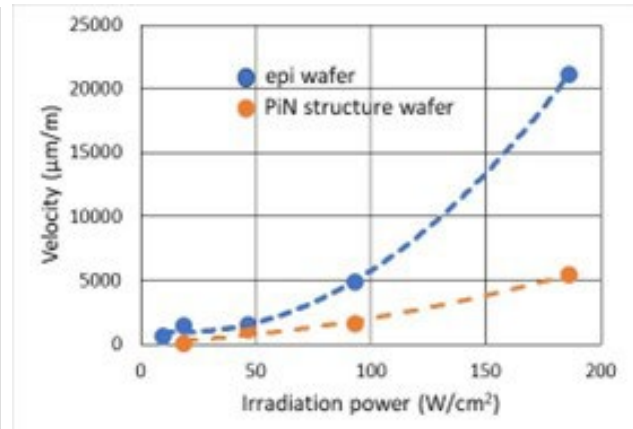
Fig. 9. Bar shaped SSF expansion at 186 W/cm^2 

Fig. 10. Glide velocity of bar shaped SSF by UV

On the other hand, PiN diodes on the wafer were forward biased by accelerated pulsed current, and the PiN diode showed the emission with a blue wavelength according to the band gap (see Fig. 11a). The length of the SSF was measured by the UVPL method from the position of the Si(g) core partials visible through the gap between the comb line patterns (see Fig. 11(b)), which aligned with the step flow direction $[1\ 1\ -2\ 0]$ of the SiC epi-wafer.

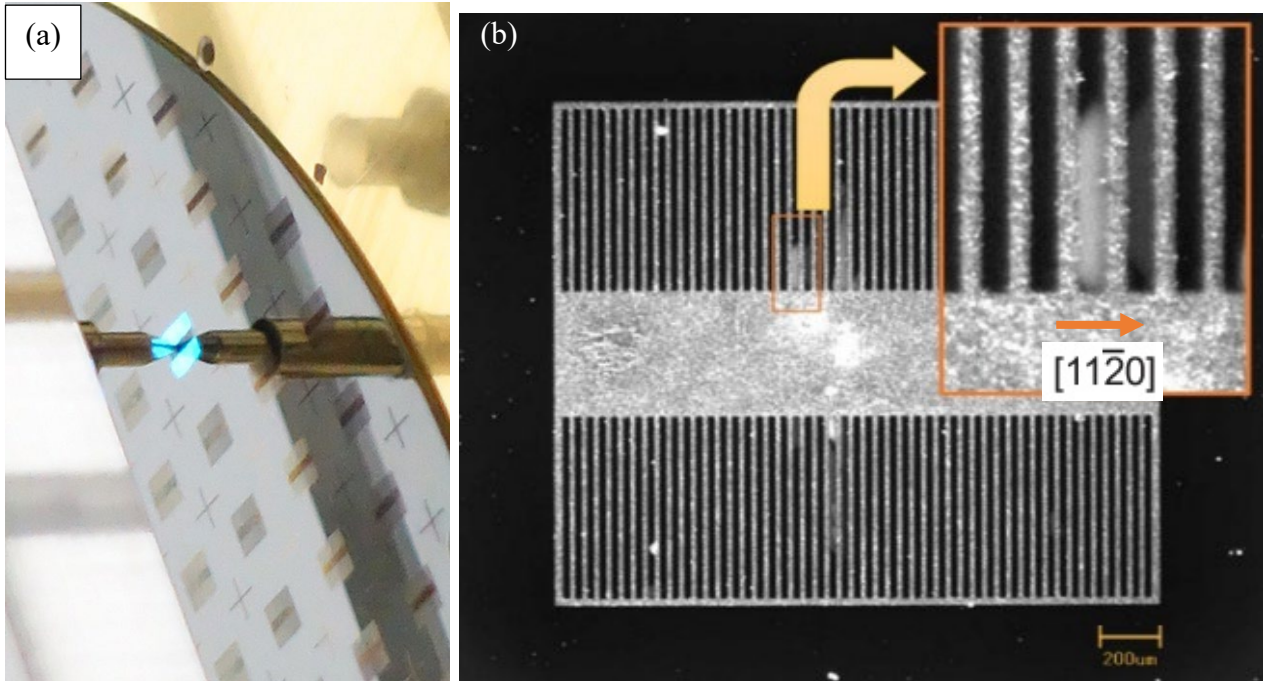


Fig. 11. (a) An emitted PiN diode by energized, (b) UVPL image of a PiN diode through BPF (420 nm) after energized

IV characteristics after accelerated current stress shows an increase in current in the recombination (low voltage) region (see Fig. 12). The initial sample already showed a high recombination current because the wafer seemed to have exceptionally high density of defects that act as recombination centers in this experiment. Fig. 13 shows the calculated glide velocity of 30° Si(g) core partials against three levels of current density.

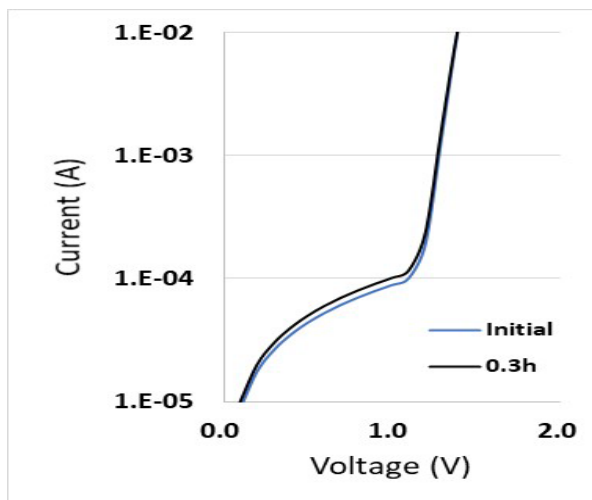


Fig. 12. IV-curve of PiN diode

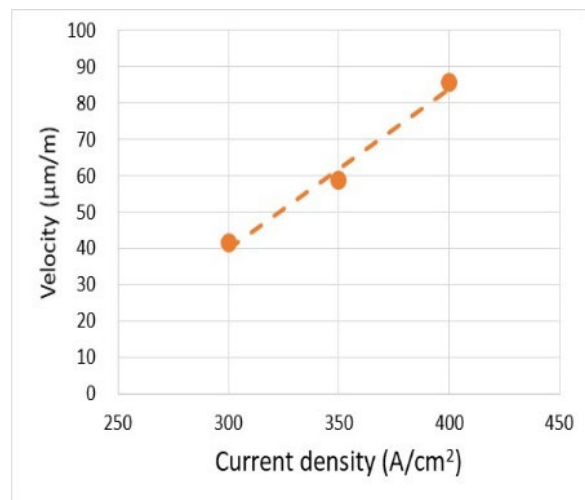


Fig. 13. Glide velocity of bar shaped SSF by current

Summary

The UV irradiance and current density can be quantitatively correlated from Fig.10 and Fig.13. 400 A/cm² of current density, for example, corresponds to 28 W/cm² of UV irradiation.

In this study, UV irradiance was correlated directly with the amount of current density, but quantification will become more versatile by correlating UV irradiance with the hole concentration at the epi/substrate interface derived from the wafer profile and current density [6].

References

- [1] K. Takano and Y. Igarashi, presented at the European Conference on Silicon Carbide and related Materials, Tours, 2021 (will be published).
- [2] T. Kimoto and H. Watanabe, *Appl. Phys. Express* 13, 120101 (2020).
- [3] T. Ishigaki, T. Murata, K. Kinoshita, T. Morikawa, T. Oda, R. Fujita, K. Konishi, Y. Mori, A. Shima, 2019 31st International Symposium on Power Semiconductor Devices and ICs, (2019).
- [4] B. Kallinger, D. Kaminzky, P. Berwian, J. Friedrich, S. Oppel, *Mater. Sci. Forum* 924, 196 (2018).
- [5] S. Hayashi, T. Yamashita, J. Senzaki, M. Miyazato, M. Ryo, M. Miyajima, T. Kato, Y. Yonezawa, K. Kojima and H. Okumura, *Japanese J. Appl. Phys.* 57, 04FR07 (2018).
- [6] T. Tawara, S. Matsunaga, T. Fujimoto, M. Ryo, M. Miyazato, T. Miyazawa, K. Takenaka, M. Miyajima, A. Otsuki, Y. Yonezawa, T. Kato, H. Okumura, T. Kimoto, and H. Tsuchida, *J. Appl. Phys.* 123 025707 (2018).